LBL-19133
Preprint c.2

Lawrence Berkeley Laboratory

UNIVERSITY OF CALIFORNIA

Materials & Molecular Research Division

RECEIVED
LAWRENCE
BERKELEY LABORATORY
MAY 22 1985
LIBRARY AND
DOCUMENTS SECTION

Submitted to Thin Solid Films

INITIAL STAGES OF THE Pd-GaAs REACTION:
FORMATION AND DECOMPOSITION OF TERNARY PHASES

T. Sands, V.G. Keramidas, R. Gronsky
and J. Washburn

April 1985

TWO-WEEK LOAN COPY
This is a Library Circulating Copy
which may be borrowed for two weeks.

LBL-19133
c.2

Prepared for the U.S. Department of Energy under Contract DE-AC03-76SF00098

DISCLAIMER

This document was prepared as an account of work sponsored by the United States Government. While this document is believed to contain correct information, neither the United States Government nor any agency thereof, nor the Regents of the University of California, nor any of their employees, makes any warranty, express or implied, or assumes any legal responsibility for the accuracy, completeness, or usefulness of any information, apparatus, product, or process disclosed, or represents that its use would not infringe privately owned rights. Reference herein to any specific commercial product, process, or service by its trade name, trademark, manufacturer, or otherwise, does not necessarily constitute or imply its endorsement, recommendation, or favoring by the United States Government or any agency thereof, or the Regents of the University of California. The views and opinions of authors expressed herein do not necessarily state or reflect those of the United States Government or any agency thereof or the Regents of the University of California.

LBL-19133

Initial Stages of the Pd-GaAs Reaction: Formation and Decomposition of Ternary Phases

T. Sands, V.G. Keramidas, R. Gronsky, and J. Washburn

Lawrence Berkeley Laboratory
University of California
Berkeley, California 94720

April 1985

Initial Stages of the Pd-GaAs Reaction: Formation and Decomposition of Ternary Phases

T. Sands[+] and V.G. Keramidas

Bell Communications Research, Inc.

600 Mountain Avenue

Murray Hill, NJ 07974

R. Gronsky and J. Washburn

Materials and Molecular Research Division

Lawrence Berkeley Laboratory

ABSTRACT

Investigations of the metallurgical reactions occuring at metal/compound semiconductor interfaces are essential for the understanding of ohmic contact and Schottky barrier formation mechanisms. The resulting film and interface morphologies are also important for the performance of discrete devices and integrated circuits.

In this study the reactions occuring during thermal annealing of the Pd-GaAs system are investigated. Reported here are the initial stages of the Pd-GaAs reactions as studied by high-resolution transmission electron microscopy, electron diffraction and energy-dispersive analysis of x-rays. The first Pd-GaAs reaction product, observed in the low temperature range ($\lesssim$315°C), is the hexagonal ternary phase $Pd_5(GaAs)_2$ (phase I with a_0 = 0.673 nm and c_0 = 0.338 nm). The second

---

([+]work performed as a visiting Industrial Fellow at the Center for Advanced Materials, Lawrence Berkeley Laboratory, Berkeley, CA 94720)

stage of the reaction leads to the formation of a second hexagonal ternary phase, Pd_4GaAs (phase II with a_0 = 0.92 nm and c_0 = 0.370 nm), and the binary phases, Pd_2Ga and Pd_2As. The concurrent application of energy-dispersive x-ray analysis and high-resolution cross-sectional transmission electron microscopy leads to the unambiguous identification of the ternary $Pd_5(GaAs)_2$ and Pd_4GaAs phases. X-ray diffraction data alone could erroneously lead to the identification of $Pd_5(GaAs)_2$ as PdGa and of Pd_4GaAs as $PdAs_2$. In view of this source of ambiguity in previous work, the sequence of reactions in the Pd-GaAs system is reevaluated and the evolution of the film and interface morphologies is discussed.

1. INTRODUCTION

Current approaches to ohmic contact and Schottky barrier formation to III-V compound semiconductors involve, by and large, deposition of metal layers and subsequent high temperature annealing. The deposited metals often react differently with the group III and group IV elements. Preferential reactions between metal and group III elements, for example, could result in the accumulation of the group V element near the interface at low temperatures and, due to its volatility, the subsequent loss of the group V element at higher temperatures. The reacted contacts generally exhibit nonplanar interfaces and possess poor mechanical properties. Furthermore, their electrical properties are likely to be dominated by the accumulated group V element and the associated nonstoichiometry in the semiconductor near the interface.[1] In silicide contacts to silicon, on the other hand, the silicide reaction consumes the surface layer of the silicon substrate. Thus, the electrical and mechanical properties of silicide/silicon interfaces are relatively independent of the initial surface preparation, especially for silicides formed by reactive metals such as Pd and Pt.[2] In addition, since the reactions are in the solid state, control of contact morphologies can be maintained.

The advent of III-V Integrated Circuits (ICs) and new III-V compound semiconductor devices such as High Electron Mobility Transistors (HEMTs) consisting of very thin (10-200 nm) layers render the nonplanar metal/semiconductor interfaces unacceptable. Ideally, what is needed is for the deposited metal(s) to react in the solid state forming stable ternary (or quaternary) compounds containing roughly equal concentrations of the group III and group V elements.

Recently, ternary compounds with nickel (Ni_2GaAs)[3,4] and palladium (Pd_2GaAs[5,6] and possibly Pd_5GaAs[7]) have been reported. There is some ambiguity,

however, as to whether the first phases formed during the Pd-GaAs reaction are binary or ternary. X-ray diffraction results reported by Olowolafe et al[8] suggest that the phases formed by annealing 50-200nm of Pd on (100) GaAs at 250°C for 60 min. are $PdAs_2$ and PdGa. Depth profiles by Auger electron spectroscopy confirmed that both Ga and As were present in the reacted layer after the samples were annealed at 250-350° C for varying lengths of time. Zeng and Chung[9] found that the first reaction detectable by in-situ x-ray diffraction of 100nm of Pd on (100) GaAs occured during annealing at 250° C in Ar. After 30-40 min. at this temperature, the primary phase was identified as PdGa with a small amount of Pd_2Ga. Annealing at 350°C resulted in the formation of Pd_2Ga, PdGa and $PdAs_2$[9].

In contrast to the above studies, Oelhafen et al.[5] reported that the dominant phase formed during low temperature annealing treatments is a ternary phase, Pd_2GaAs. The electron diffraction pattern of this ternary phase suggested a tetragonal unit cell with a_0 = 0.481nm and c_0 = 0.582nm. No Pd-As compounds were detected. Recently, Kuan[6] has suggested that Pd_2GaAs is hexagonal with a_0 = 0.672 nm and c_0 = 0.340 nm.

All four studies agree that after annealing at moderate temperature (>350 °C), the dominant phase is PdGa, possibly due to the volatility of arsenic and its compounds at elevated temperatures.

In this study, the low temperature annealing behavior of evaporated Pd films on (100) GaAs is investigated in an effort to clarify the initial stages of the Pd-GaAs reaction.

2. EXPERIMENTAL METHODS

Palladium was deposited on (100) GaAs substrates by electron-beam evaporation. Prior to Pd deposition, the GaAs surface was prepared by immersion into a 9:1 DI H_2O:HCl solution for 10 sec. followed by a DI H_2O rinse. The surface was

blown dry with N_2. Palladium was then deposited to a thickness of 50nm at a rate of 0.6 nm/s in a vacuum of 1-2 x 10^{-6} torr. Annealing treatments were performed in flowing forming gas (95% Ar and 5% H_2). The experimentally measured thermal cycles can be described approximately by

$$T[°C] = 25 + (T_a-25)[1-\exp(-t/170)] \text{ for } 0<t<900s.$$

and

$$T[°C] = 25 + (T_a-25) \exp [(900-t)/190] \text{ for } t>900s.$$

where T_a is the maximum temperature. In subsequent sections, these annealing treatments are simply described as 10 min. at T_a[°C].

Cross-sectional transmission electron microscopy (XTEM) specimens were prepared by argon ion milling (5kV, 15° tilt, 0.5mA total gun current) with a liquid nitrogen cooled stage. Preparation of plan-view specimens was accomplished by etching away the GaAs substrate from the back side with chlorine gas dissolved in methanol. A JEOL 200CX electron microscope equipped with an ultra-high resolution pole piece was employed for cross-sectional work. Plan-view specimens were examined in a Siemens 102 TEM. Energy dispersive spectrometry (EDS) of x-rays was performed with a Kevex model 3400 ultra-thin-window spectrometer on a JEOL 200CX TEM/STEM. A GaAs standard was used for partial quantification of the EDS spectra. However, since a reliable Pd-Ga standard was not available, the [Pd]:[Ga] ratios reported below are tentative.

Several TEM specimens from each sample were studied in both plan-view and cross-section in an effort to provide interpretations which are representative of the "average" behavior.

3. RESULTS

3.1 As-deposited

Figure 1(a) is a cross-sectional image of the as-deposited sample. It is clear from this image that the Pd-GaAs reaction begins during deposition. Note that the native oxide (white band) remains intact. A high resolution image

of the reacted layer below the native oxide is shown in Figure 2. The grains of the reacted phase are ∿6nm thick and ∿20nm wide. There is a high degree of texture as indicated by the inset optical diffraction pattern. This pattern and results presented below suggest that the first phase (designated as phase I) is hexagonal with

$$\langle 0001 \rangle_I \;//\; \langle 011 \rangle_{GaAs}$$

and

$$\{ 2\bar{1}\bar{1}0 \}_I \;//\; \{ 100 \}_{GaAs}.$$

The orientations of the grains of phase I differ by rotations of a few degrees about <0001>. Note that <0001> is parallel to only one of the two possible <011> directions in the plane of the substrate surface.

3.2 <u>220°C, 10 min.</u>

After annealing at 220°C for 10 minutes the layer of phase I has thickened to ∿10nm and the native oxide has been dispersed. Figure 1(b) also shows that voids have formed at the Pd/phase I interface. These voids are 15 nm in diameter and are separated by ∿50 nm.

The layer of phase I in $\langle 0\bar{1}10 \rangle$ zone-axis orientation is shown in Fig. 3. The diffraction pattern confirms the orientation relationship presented above. As a further check, the plan-view diffraction pattern (Fig. 4(b)) shows that phase I is in $\langle 2\bar{1}\bar{1}0 \rangle$ zone-axis orientation (i.e. $\langle 2\bar{1}\bar{1}0 \rangle_I \;//\; \langle 100 \rangle_{GaAs}$). From observations of phase I in the three major zone-axis orientations in the presence of unreacted Pd and GaAs as internal standards, the lattice parameters of phase I are

$$a_0 = 0.673 \pm 0.002 \text{ nm}$$

and

$$c_0 = 0.338 \pm 0.001 \text{ nm}.$$

3.3 275°C, 10 min.

The reacted layer in the sample annealed at 275° C for 10 min. was found to be laterally nonuniform (Fig. 5(a)). A majority of the film consists of phase I with a surface layer of unreacted Pd. However, in some highly localized areas of the film the Pd was completely consumed. These deep penetrations were found to contain a second hexagonal phase (designated as phase II) with

$$a_0 = 0.92 \pm 0.01\text{nm}$$

and

$$c_0 = 0.370 \pm 0.005 \text{ nm}.$$

Phase II exhibits a well-defined orientation relationship with GaAs,

$$\langle 0001 \rangle_{II} \;//\; \langle 011 \rangle_{GaAs}$$

and

$$\{\bar{2}\bar{1}30\}_{II} \;//\; \{100\}_{GaAs},$$

at this annealing temperature. This orientation relationship is illustrated by the image of a phase II/GaAs interface in Fig. 6(b). Analysis of EDS spectra obtained from cross-sectional samples with a 10nm diameter probe suggests the nominal compositions, $Pd_5(GaAs)_2$ for phase I and Pd_4GaAs for phase II. Note that the composition Pd_2GaAs was reported by Oelhafen et al[5] for a tetragonal phase and by Kuan[6] for a hexagonal phase with nearly identical lattice parameters.

3.4 315° C, 10 min.

Annealing at 315° C for 10 min. also results in a laterally nonuniform film morphology (Figs. 4(c) and 5(b)). Only trace amounts of unreacted Pd remain. Figure 7 shows that the thinner regions of the film consist of 15-30 nm of phase I. The thicker penetrations spaced ∿1μm apart (Fig. 8) were found to consist of phase II and two additional phases, III and IV.

Phase III, observed in small amounts adjacent to the GaAs in the deepest penetrations of the reacted films , has orthogonal planes with spacings d_1 = 0.55 ± 0.02nm and d_2 = 0.41 ± 0.01nm. These plane spacings are consistent with those of orthorhombic Pd_2Ga (a_o = 0.7814nm, b_o = 0.5493nm, c_o = 0.4046nm).[10] The identification of phase III as Pd_2Ga is corroborated by the fact that Pd_2Ga was reported in x-ray diffraction studies of samples annealed under similar conditions.[8,9] The planes with spacing 0.41nm were found to be parallel to the $\{01\bar{1}\}$ planes of the GaAs substrate (Fig. 8(c)) suggesting the orientation relationship:

$$\langle 001\rangle_{Pd_2Ga} \;//\; \langle 01\bar{1}\rangle_{GaAs}$$

$$\{010\}_{Pd_2Ga} \;//\; \{100\}_{GaAs}.$$

Inclusions of a fourth phase, phase IV, were usually found adjacent to or directly above the Pd_2Ga. Two grains of phase IV are visible in Figs. 8(a) and (b). One grain exhibits fringes of spacing 0.55 ± 0.02nm at an angle of 71° to fringes of spacing 0.52 ± 0.02nm. A second grain shows fringes of spacing 0.83 ± 0.02nm (see Fig. 8(a)). These interplanar spacings and angles are consistent with those of monoclinic Pd_2As (a_o = 0.924nm, b_o = 0.847nm, c_o = 1.045nm and β = 94).[11] Analyses of similar grains in different regions of the film were in agreement with this conclusion. Of course, the possible incorporation of significant amounts of Ga in the Pd_2As (and As in the Pd_2Ga) cannot be excluded since these phase identifications are based on structural information only.

Figure 9 contains EDS spectra obtained from phases I and II in a plan-view sample. Analysis of the spectra in Figs. 9(a) and (b) indicates that the film contains less arsenic than gallium. Averaging over several spectra, the [As]:[Ga] ratio is estimated to be 0.8 ± 0.1.

3.5. 410°C, 10 min.

The morphology of the sample annealed at 410°C (Fig. 4(e)) is similar to the morphology of the sample annealed at 315°C except that phase I was not detected. Electron diffraction results suggest that the film consists primarily of phase II and possibly small amounts of the binary compounds Pd_2Ga and PdGa. Analysis of EDS data yields an average film composition of [Pd]:[Ga]:[As]$\cong$5:2:1, consistent with a two-phase microstructure of Pd_4GaAs and PdGa. A complete analysis of the phase distribution was difficult due to high stresses at the Pd-Ga-As/GaAs interface which resulted in fracture of the GaAs near the interface in cross-sectional TEM samples. These stresses (tensile in the reacted film) are probably due to a difference between the thermal expansion coefficients of the reacted film and the GaAs substrate.

3.6 480°C, 10 min.

During annealing at 480°C for 10 min., the reacted layer is partially converted to Pd-Ga phases. However, some patches of phase II in contact with the GaAs substrate remain. Figure 9 contains EDS spectra from a grain of arsenic-depleted phase II (Fig. 9(d)) and a grain of a Pd-Ga compound (Fig. 9(c)). The average [As]:[Ga] ratio in this film was found to be 0.2 $\pm$ 0.1. Figure 10 shows that the reaction to form the Pd-Ga compounds is accompanied by the formation of pits in the sample surface at grain boundaries in the reacted film (these pits are also visible in Fig. 4(e) after annealing at 410°C) and voids in the GaAs at the Pd-Ga/GaAs interface.

The identification of the Pd-Ga compound in these samples as cubic PdGa is questionable in view of electron diffraction results. Several diffraction patterns from grains of the dominant Pd-Ga phase (e.g. Fig. 10(c)) reveal diffracting planes with spacings 0.348, 0.284, 0.224, 0.200, 0.166 and 0.134 nm which

correspond quite well with the plane spacings 0.346, 0.282, 0.219, 0.200, 0.163 and 0.131 nm of cubic PdGa.[12] However, the measured angles between diffracting planes are not compatible with cubic symmetry. Further experiments are underway to resolve this discrepency.

The observations described in this section are summarized in Table 1.

4. DISCUSSION

4.1 Relationship to Previous Studies

In a previous section, phase I was shown to be hexagonal with a_0 = 0.673 nm and c_0 = 0.338nm. Under similar annealing conditions, however, Oelhafen *et al*[5] reported the formation of a tetragonal phase with nominal composition Pd_2GaAs and lattice parameters a_0 = 0.481nm and c_0 = 0.582nm. Figure 11 is a schematic diagram of the diffraction pattern expected from a plan-view specimen of this tetragonal phase (substrate normal [100]) with the orientation relationship reported by Oelhafen *et al*. A nearly identical diffraction pattern is obtained from a thin film of phase I on (100) GaAs (Fig. 4(b)). In Fig. 11 the diffraction spots from the ternary phase are indexed in terms of both the tetragonal and hexagonal unit cells. It is apparent that the patterns have the correspondence

$$d_{0110,I}(0.583\text{nm}) \cong d_{001,tet.}(0.582\text{nm})$$

and

$$d_{0001,I}(0.338\text{nm}) \cong d_{110,tet.}(0.354\text{nm}).$$

It appears that the tetragonal phase reported by Oelhafen *et al* and the hexagonal phase I (also reported by Kuan)[6] are actually the same. Diffraction patterns from cross-sectional samples obtained in this study and shown in Figs. 2,3,6(a) and 7 strongly suggest that a hexagonal unit cell is more appropriate.

In contrast with the results reported here and the data of Oelhafen *et al*, the observations of Zeng and Chung[9] suggest that the first phase to form during

annealing at 250° C is PdGa with a small amount of Pd_2Ga. Zeng and Chung employed *in situ* x-ray diffraction for phase identification. Use of this technique alone can lead to ambiguous results if two compounds have overlapping diffraction peaks. The calculated peak positions for PdGa and phase I are compared in Table 2. Because phase I is hexagonal with $c_0/a_0 \cong 0.5$, the relative positions of the diffraction peaks, especially if only a few peaks are detected, can lead to the mistaken conclusion that phase I is cubic with $a_0 \cong 0.5$ nm. It is possible that Zeng and Chung[9] have misinterpreted their data in this way. For example, Fig. 1 of ref. 9 (250°C for 35-40 min.) shows a peak labeled PdGa (210) approximately 0.9 + 0.1° (in units of 2θ) from the peak labeled Pd(111). The calculated angular separation between PdGa(210) and Pd(111) (assuming a_0[PdGa] = 0.489 nm [12], a_0[Pd] = 0.38898 nm[13] and [CuKα] = 0.1542 nm) is 1.13°. A satisfactory match with the observed angular separation is also achieved by indexing the unknown peak as due to diffraction from the $\{02\bar{2}1\}$ and $\{1\bar{3}20\}$ planes of phase I. In this case the calculated angular separation is 0.7°. A similar interpretation of the low temperature results of Olowolafe *et al*[8] may be appropriate.

After annealing for 40 min. at 350°C, Olowolafe *et al*[8] detected $PdAs_2$, PdGa and Pd_2Ga. The x-ray diffraction pattern from this specimen (Fig. 1 in ref. 8) contains six peaks which were attributed solely to cubic $PdAs_2$ with a_0 = 0.5982 nm.[14] Zeng and Chung[9] recorded a similar pattern for a sample annealed for 15-20 min. at 350 °C (Fig. 1 of ref. 9). As illustrated in Table 3, all peaks solely attributed to $PdAs_2$ can also be attributed to phase II, the hexagonal ternary phase with a composition of approximately Pd_4GaAs. Furthermore, XTEM images of samples annealed at 350 °C show that phase II is the dominant phase.[15]

While these results tend to suggest that some earlier interpretations of x-ray data may be in error, differing annealing times, temperatures and ambients

may, of course, result in different phases. For example, it is possible, that the identification of PdGa as the first phase (detectable by x-ray diffraction) may be correct for the annealing conditions used by Zeng and Chung.[9] However, it is clear that considering only binary phases in a ternary system can lead to errors in the interpretation of x-ray diffraction spectra.

4.2 Morphological Development of the Ternary Phases

The first evidence of the Pd-GaAs reaction is apparent in the as-deposited state. That the first product of the Pd-GaAs reaction (phase I) forms beneath the native oxide suggests that Pd is the dominant moving species at low temperatures. However, the concentrations of Ga and As atoms in the ternary phase I are approximately thirty percent lower than the concentrations of Ga and As in GaAs (assuming a composition of $Pd_5(GaAs)_2$ and a unit cell content of one formula unit for phase I). Consequently, the mechanical dispersion of the native oxide begins in the early stages of the reaction. Phase I exhibits a well-defined orientation relationship with (100) GaAs, possibly because the misfit between the $\{0\bar{3}30\}$ planes of phase I and the $\{022\}$ planes of GaAs is only three percent.

The presence of voids in the Pd adjacent to the Pd/phase I interface indicates that Pd is still the dominant moving species during the early stages of the reaction at 220° C. It is likely that the voids result from the preferential depletion of Pd from triple points or grain boundary intersections. Thus, the transport of Pd to the phase I layer occurs primarily by surface diffusion.

As the reaction continues, the growth of the phase I layer is probably limited by diffusion of Pd through the reacted layer, especially since phase I is predominantly monocrystalline. The positions of the deep penetrations of the

Pd-rich ternary phase (phase II) in the samples annealed at higher temperatures ($\gtrsim$ 250 °C) probably correspond to areas in the phase I film which contain fast diffusion paths (eg. cracks, pores, thin areas or large-angle grain boundaries). Indeed, grains of phase I with random orientation were sometimes found adjacent to the deepest penetrations. The formation of phase II in these areas with fast diffusion paths (separated by ∿1μm) is accompanied by significant lateral surface diffusion of Pd. The large change in Ga and As concentrations (a reduction of 50 percent from GaAs to phase II, assuming a composition of Pd_4GaAs and a unit cell content of three formula units) also contributes to the "bulging" appearance of the deep penetrations (Fig. 5).

In the sample annealed at 315° C for 10 min., small amounts of the binary phases, Pd_2Ga and possibly Pd_2As, were found at the interface between phase II and GaAs. However, in the samples annealed at 410° C for 10 min. and 350° C for 100 min.,[15] phase II was found to be the dominant phase in direct contact with the GaAs substrate. These observations suggest that, at the lower annealing temperatures, phase II decomposes into the binary phases Pd_2Ga and Pd_2As at the interface with GaAs. This decomposition reaction may be driven by a reduction in excess interfacial free energy due to the excellent lattice match between the (010) plane of Pd_2Ga and the (100) plane of GaAs ($d_{200}[Pd_2Ga]$ = 0.391nm, $d_{001}[Pd_2Ga]$ = 0.405nm and d_{011} [GaAs]=0.3997 nm). A more thorough understanding of the relative stabilities of these phases in the presence of the GaAs substrate will require the accurate determination of compositions by comparison of energy dispersive x-ray spectra with spectra from known standards containing Pd.

The sequence of reactions described above is illustrated schematically in Fig. 12. At higher temperatures ($\gtrsim$ 400 °C), the interaction between the reacted film and the annealing ambient becomes strong, resulting in the depletion of

arsenic from the phase II film. This reaction can be described as Pd_4GaAs + 3 GaAs → 4 PdGa + 4 As↑ It is interesting to note that this reaction involves the further consumption of the GaAs substrate as evidenced by the presence of voids at the Pd-Ga/GaAs interface (Fig. 10(a)). The formation of surface pits at grain boundaries in the reacted film indicates that grain boundaries play a dominant role in the transport of arsenic.

Finally, the results of this study suggest that the sequence of phase formation during the Pd/GaAs reaction will most likely depend not only on the annealing temperature and ambient, but on the amount of Pd deposited as well. For example, the formation of phase II would not be expected during annealing of less than 20nm of Pd on GaAs at temperatures below ∿250°C since the Pd would be completely consumed by the rapid formation of a thin layer of phase I, considering that it has already nucleated in the as-deposited state. This argument is further supported by Oelhafen et al's[5] observation that $PdAs_2$ was not detected after annealing 15 nm of Pd on GaAs under various conditions, even though other workers[8,9] had observed $PdAs_2$ in their studies of thicker Pd films on GaAs. (Recall that phase II has probably been mistakenly identified as $PdAs_2$ in previous studies).

5. SUMMARY

The initial stages of the Pd-GaAs reaction have been investigated by depositing thin (50 nm) films of Pd on (100) GaAs followed by annealing at low temperatures (<500°C). An important observation is that Pd readily penetrates the native oxide on GaAs during deposition at room temperature. This leads us to conclude that when Pd is involved, ultra-high vacuum conditions may not be necessary for the GaAs surface preparation. From a structural point of view it is evident that thin films of Pd (≲ 20 nm) on (100) GaAs, when annealed at

low temperatures ($\lesssim$ 250°C) will yield adherent and nominally monocrystalline thin films of the ternary phase I, $Pd_5(GaAs)_2$. The structural and compositional "simplicity" of the $Pd_5(GaAs)_2$/GaAs interface, across which the [As]:[Ga] ratio is approximately one, as well as the planarity of the interface suggest that such films in combination with diffusion barriers may be ideal for generating shallow electrically active metal/GaAs interfaces. Phase II, Pd_4GaAs, may find similar application if uniform films can be fabricated. However, the thermal stabilities of $Pd_5(GaAs)_2$ and Pd_4GaAs as well as the electrical properties of the interfaces will ultimately determine the applicability of such phases as contact materials.

ACKNOWLEDGEMENTS

The authors would like to thank the staff of the National Center for Electron Microscopy, Lawrence Berkeley Laboratory, and Ariel Dori of Bell Laboratories for technical assistance. One of the authors (T.S.) wishes to acknowledge Dr. T.R. Dinger and C. Echer for expert assistance with the EDS measurements and Ms. G. King for aiding in the preparation of TEM specimens. Many valuable discussions with Professor M-A. Nicolet of the California Institute of Technology are also gratefully acknowledged.

This work was supported by the Director, Office of Energy Research, Office of Basic Energy Sciences, Materials Science Division of the U.S. Department of Energy under Contract No. DE-AC03-76SF00098.

REFERENCES

1. J.L. Freeouf and J.M. Woodall, Appl. Phys. Lett., 39 (1981) 727.
2. K.N. Tu and J.W. Mayer, in Thin Films-Interdiffusion and Reactions, edited by J.M. Poate, K.N. Tu and J.W. Mayer (Wiley, New York, 1978) p. 361.
3. M. Ogawa, Thin Solid Films, 70 (1980) 181.
4. A. Lahav and M. Eizenberg, Appl. Phys. Lett., 45 (1984) 256.
5. P. Oelhafen, J.L. Freeouf, T.S. Kuan, T.N. Jackson and P.E. Batson, J. Vac. Sci. Technol., B1 (1983) 588.
6. T.S. Kuan, Mat. Res. Soc. Symp. Proc. Vol. 31 (1984) 143.
7. J.P. Delrue, M. Wittmer, T.S. Kuan and R. Ludeke, Mat. Res. Soc. Symp. Proc; Layered Structures, Epitaxy and Interfaces, 1984 Fall Meeting, in press.
8. J.O. Olowolafe, P.S. Ho, M.J. Hovel, J.E. Lewis and J.M. Woodall, J. Appl. Phys., 50 (1979) 955.
9. X-F. Zeng and D.D.L. Chung, J. Vac. Sci. Technol., 21 (1982) 611.
10. K. Schubert, H.L. Lukas, H.G. Meissner, and S. Bhan, Z. Metallk., 50 (1959) 534.
11. Powder Diffraction File (JCPDS International Centre for Diffraction Data, Swarthmore, Penn., 1980) 17-227.
12. E. Hellner and F. Laves, Z. Naturforsch., 2a (1947) 177.
13. Powder Diffraction File (JCPDS International Centre for Diffraction Data, Swarthmore, Penn., 1980) 5-0681.
14. L. Thomassen, Z. physik. Chem., B4 (1929) 279.
15. K.M. Yu and T. Sands, unpublished.

TABLE 1

Reactions during annealing
50nm of Pd on (100) GaAs

Initiation* temperature	Reaction	Morphology
as-deposited	$5Pd + 2GaAs \rightarrow Pd_5(GaAs)_2$	Results in uniform and highly textured $Pd_5(GaAs)_2$ layer. Voids form in Pd at $Pd/Pd_5(GaAs)_2$ interface.
~250°C	$4Pd + GaAs \rightarrow Pd_4GaAs$ (also $3Pd + Pd_5(GaAs)_2 \rightarrow 2Pd_4GaAs$)	Pd_4GaAs formed in vicinity of fast diffusion paths in $Pd_5(GaAs)_2$ film. Lateral surface diffusion of Pd is significant.
~300°C	$Pd_4GaAs \rightarrow Pd_2Ga + Pd_2As$	Decomposition is localized to $Pd_4GaAs/GaAs$ interface. Pd_2Ga is epitaxial with GaAs.
~400°C	$Pd_4GaAs + 3GaAs \rightarrow 4PdGa + 4As\uparrow$	Localized reaction results in i) voids in GaAs at interface and ii) pits in surface at grain boundaries in reacted film.

*"Initiation temperature" is the approximate temperature at which reaction products (detectable by high-resolution TEM in cross-section) appear after annealing for 10 min.

TABLE 2

Comparison of PdGa and phase I plane spacings*

PdGa			Phase I		
indicies	plane spacing [nm]	2θ [degrees]	indicies	plane spacing [nm]	2θ [degrees]
			$0\bar{1}10$	0.583	15.2
001	0.489	18.1			
110	0.346	25.8	$0001,2\bar{1}\bar{1}0$	0.338	26.4
111	0.282	31.7	$01\bar{1}1,2\bar{2}00$	0.292	30.6
002	0.245	36.8	$2\bar{1}\bar{1}1$	0.239	37.6
210	0.219	41.3	$02\bar{2}1,1\bar{3}20$	0.221	40.9
211	0.200	45.4	$03\bar{3}0$	0.194	46.8
220	0.173	53.0	$0002,03\bar{3}1,$ $4\bar{2}\bar{2}0$	0.168	54.6
003	0.163	56.5	$3\bar{4}10,01\bar{1}2$	0.162	56.8
310	0.155	59.8	$2\bar{1}12,4\bar{2}\bar{2}1$	0.150	61.9
311	0.147	63.1	$02\bar{2}2,4\bar{4}00$	0.146	63.8

*calculated assuming CuK α = 0.1542 nm and a_0[PdGa] = 0.489nm [12].

TABLE 3

Comparison of diffraction peak positions for $PdAs_2$ and phase II*

Approximate peak position (2θ) measured from Fig. 1 of [8]	indexing based on $PdAs_2$[8]	calculated 2θ for $PdAs_2$	possible indexing as phase II	calculated 2θ for phase II
26.6 ± 0.2	111	25.8	$0\bar{1}11$	26.6
30.8 ± 0.2	200	29.9	$2\bar{1}\bar{1}1$	31.0
33.5 ± 0.2	212	45.5	$0\bar{2}21$	33.0
+36.5 ± 0.2	211	36.8	--	--
50.7 ± 0.2	311	50.6	$0\bar{1}12$	50.7
70.0 ± 0.2	420	70.4	$0\bar{4}42$	69.4
+72.3 ± 0.2	421	72.4	--	--
73.9 ± 0.2	332	74.4	$2\bar{7}50$	74.5

* assuming CuKα radiation (λ= 0.1542nm) and $a_0[PdAs_2]$ = 0.5982nm [14].

\+ peak overlaps with 200 PdGa

\+ peak overlaps with 321 PdGa

FIGURE CAPTIONS

1. Cross-sectional TEM images of the (a) as-deposited sample and (b) a sample annealed at 220°C for 10 min. Scales are the same for both micrographs.
2. Higher magnification image of the interfacial region in the as-deposited sample. An optical diffraction pattern from the negative shows that phase I is in <0001> zone-axis orientation.
3. Higher magnification image of the interfacial region in the sample annealed at 220°C for 10 min. The inset diffraction pattern shows that $\langle 0001 \rangle_I$ is parallel to $\langle 011 \rangle_{GaAs}$. Moiré fringes are visible at the phase I/GaAs interface.
4. Low magnification TEM images and corresponding diffraction patterns from plan view specimens of samples annealed for 10 min. at (a,b) 220°C, (c,d) 315°C and (e,f) 410°C. The diffraction pattern in (b) is the superposition of the polycrystalline Pd ring pattern and the monocrystalline phase I spot pattern ($\langle 2\bar{1}\bar{1}0 \rangle$ zone-axis orientation). Diffraction spots from phases I and II are visible in (d). Figure (f) shows strong spots from phase II and Pd_2Ga.
5. Cross-sectional images of samples annealed at (a) 275°C and (b) 315°C for 10 minutes. Compare the image in (b) with the plan-view image from the same sample (Fig. 4(c)).
6. Cross-sectional HREM images of (a) the phase I/GaAs and (b) phase II/GaAs interfaces. Samples were annealed at 275°C and 350°C, respectively. The images and their corresponding electron diffraction patterns illustrate the orientation relationships described in Section 3. Gallium arsenide is in <011> zone-axis orientation. Phases I and II are in <0001> zone-axis orientation.

7. Cross-sectional HREM image of the thin phase I layer between the deep penetrations in the sample annealed at 315°C for 10 min. The image in (b) is similar to the image in Fig. 3 except that no unreacted Pd remains. Note that (b) is an enlarged image of the boxed region in (a).
8. Cross-sectional HREM image of a deep penetration in the sample annealed at 315°C for 10 min. The images in (b) and (c) are enlarged from the boxed regions in (a). The micrograph in (a) shows the generally observed layered seqence of phases, phase II/Pd_2As/Pd_2Ga/GaAs.
9. Energy dispersive x-ray spectra from (a) phase I and (b) phase II after annealing at 315°C and from (c) Pd-Ga and (d) phase II after annealing at 480°C. The copper peak is an artifact due primarily to backscattered electrons striking the copper specimen grid.
10. Cross-sectional TEM images of the PdGa/GaAs interface after annealing at 480°C. Surface pits and interface voids are visible in (a). High-resolution image of the PdGa/GaAs interface is shown in (b). Arrowed diffraction spot in (c) arises from planes of spacing 0.2 nm in PdGa (indicated by arrow in (b)). As described in section 3.6, the identification of the Pd-Ga compound as PdGa is tentative.
11. Schematic diffraction patterns from GaAs ("g"); the hexagonal phase I ("h") and the tetragonal phase ("t") reported by Oelhafen et al.[5] The diffraction spots from the tetragonal and hexagonal phases overlap. However, only the hexagonal unit cell is consistent with diffraction patterns from cross-sectional samples (see Figs. 1, 3, 6 and 7).
12. Schematic diagram of the morphological evolution of the Pd-GaAs system during low temperature annealing treatments. The sequence of reactions is described

in section 4.2. The final states of the reacted films after 10 min. annealing treatments at 220, 275 and 315°C are indicated.

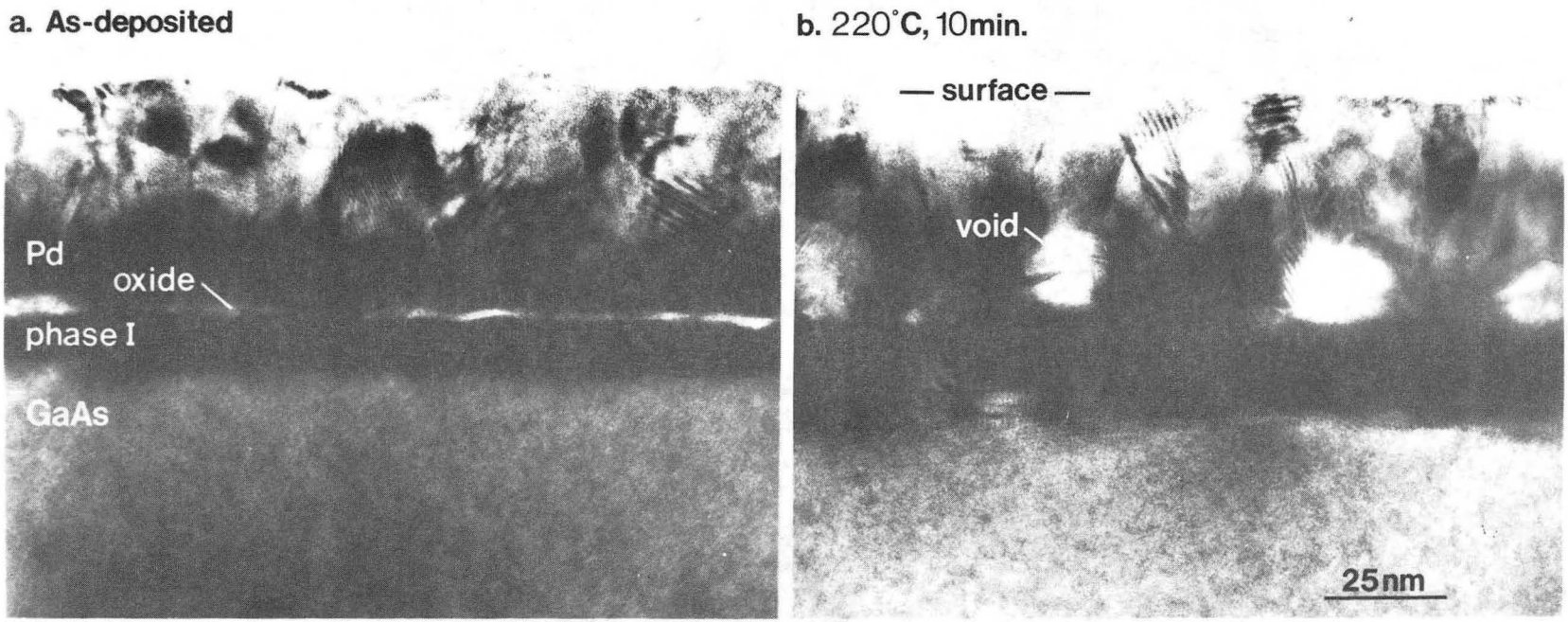

XBB 852-1078

Fig. 1

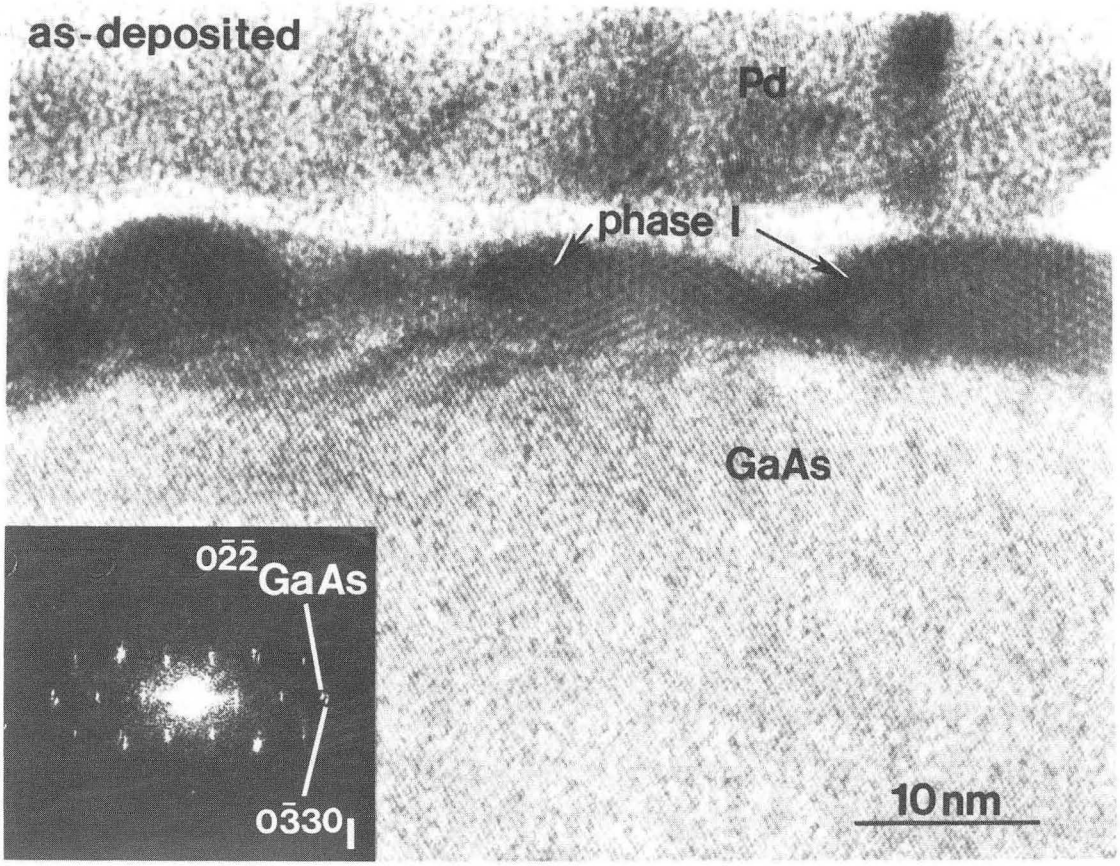

XBB 852-1076

Fig. 2

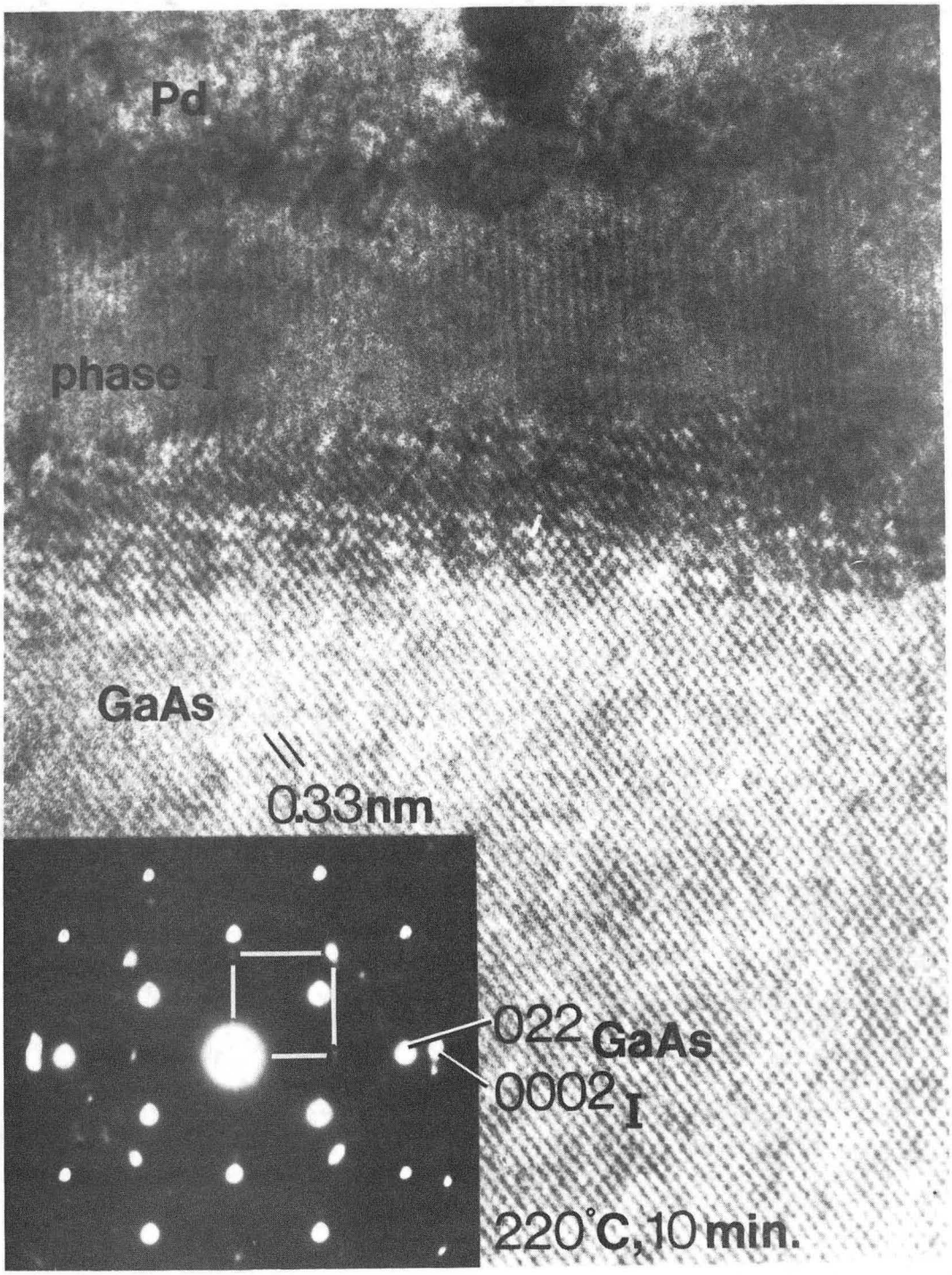

XBB 852-1077

Fig. 3

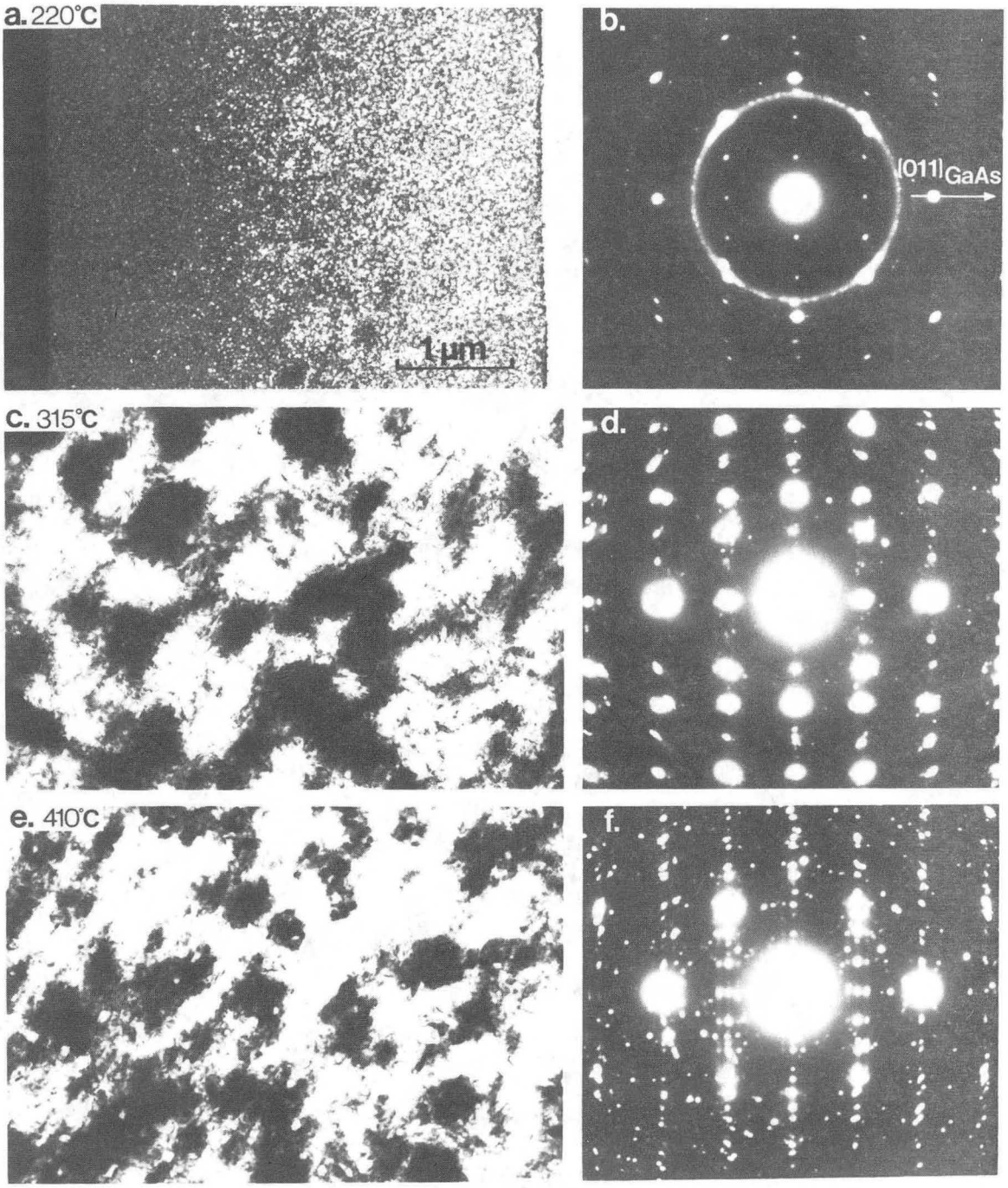

XBB 852-1329

Fig. 4

a. 275 °C, 10 min.

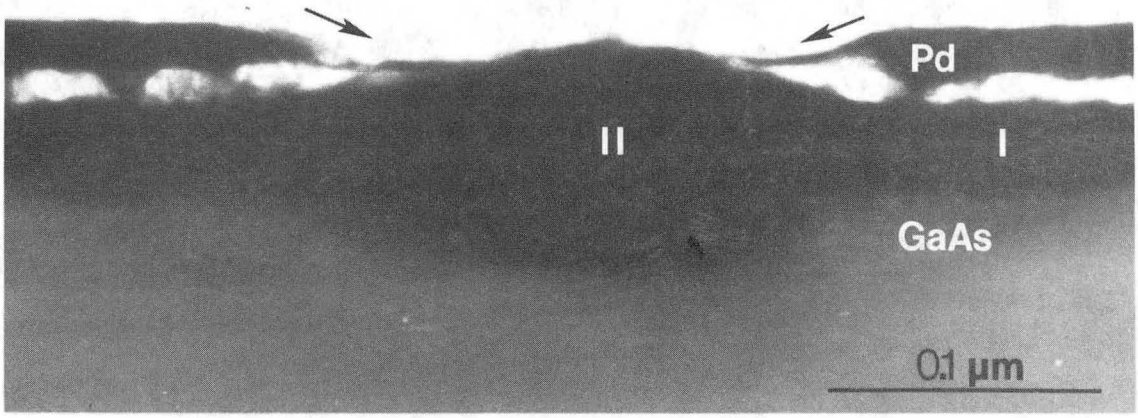

b. 315 °C, 10 min.

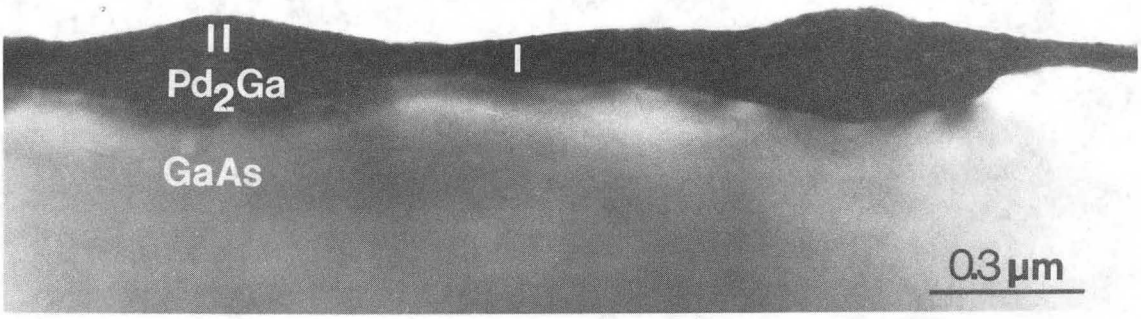

XBB 853-1996

Fig. 5

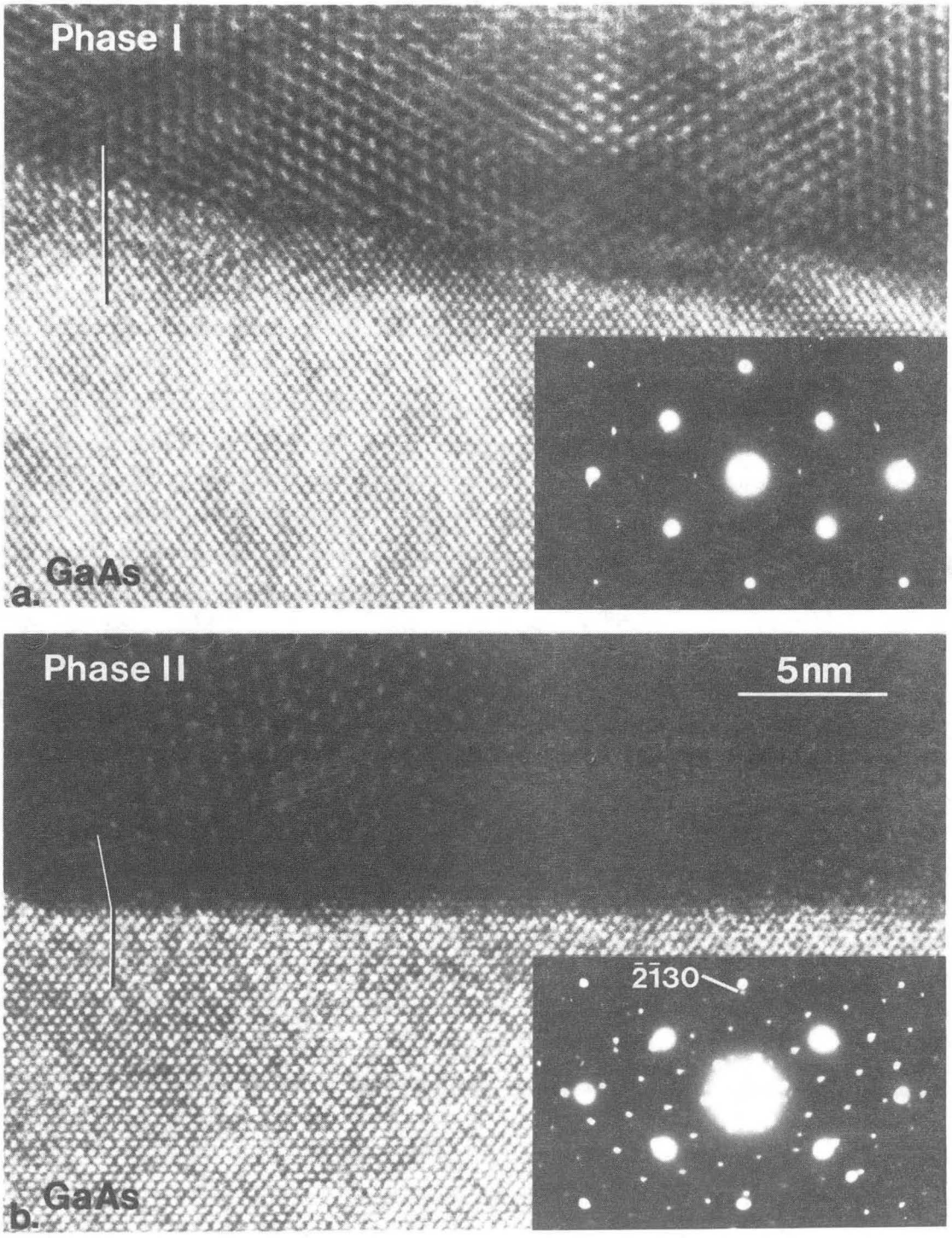

XBB 853-1997

Fig. 6

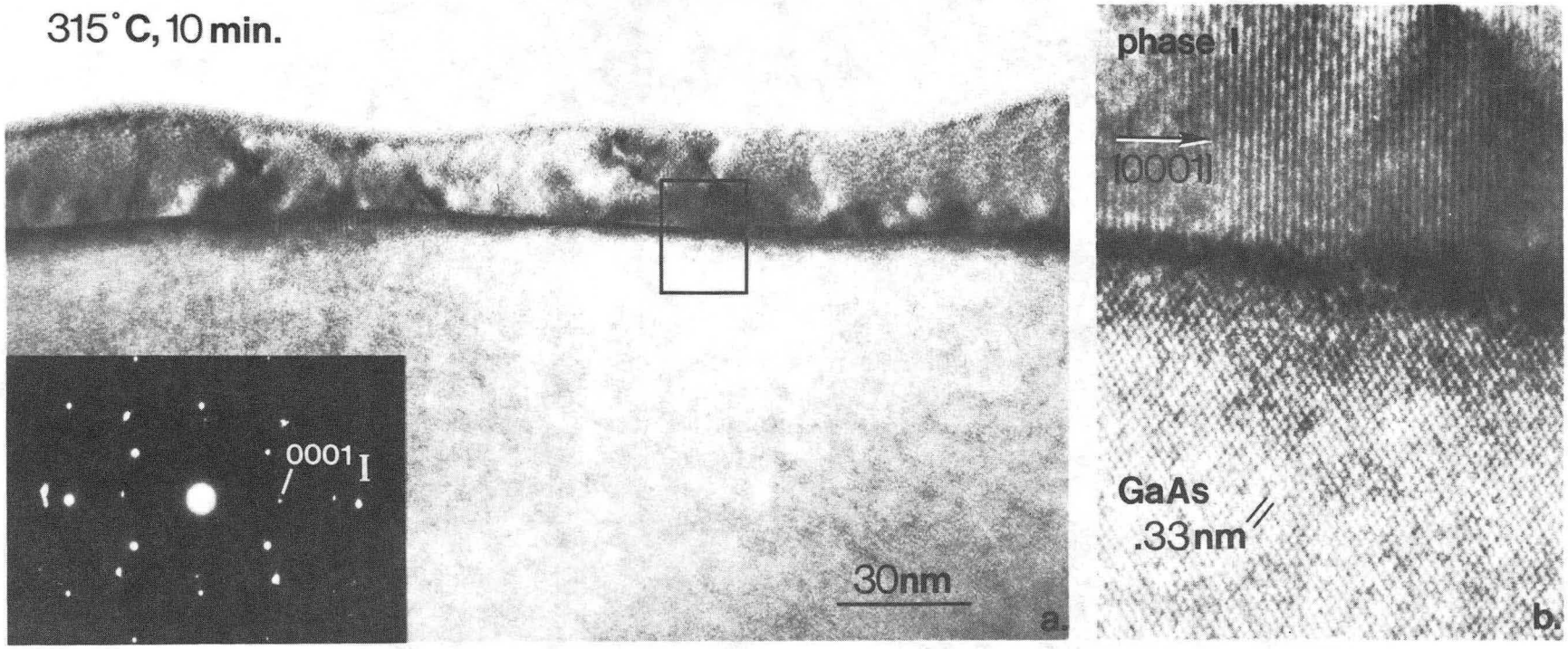

XBB 852-1327

Fig. 7

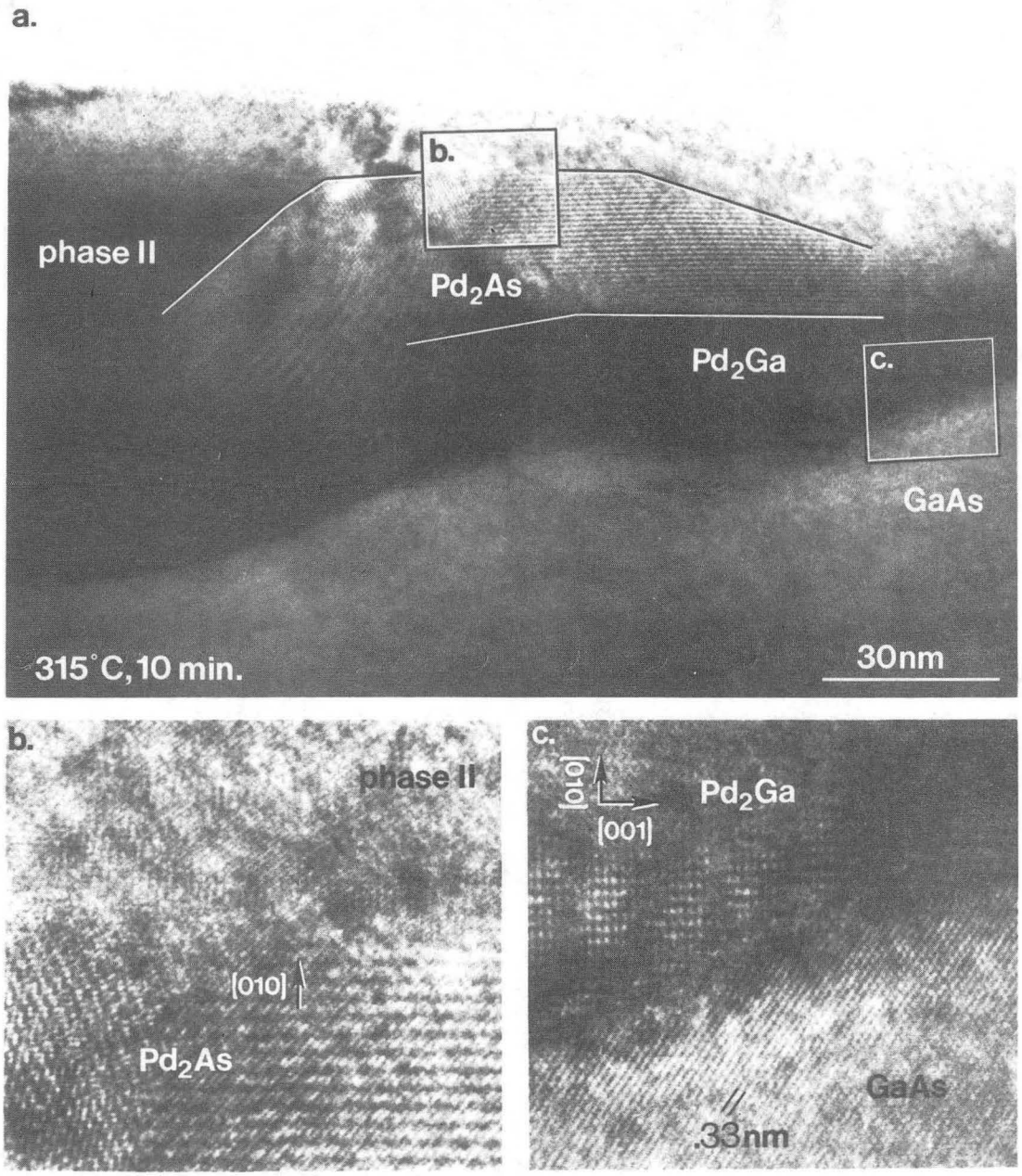

XBB 852-1328

Fig. 8

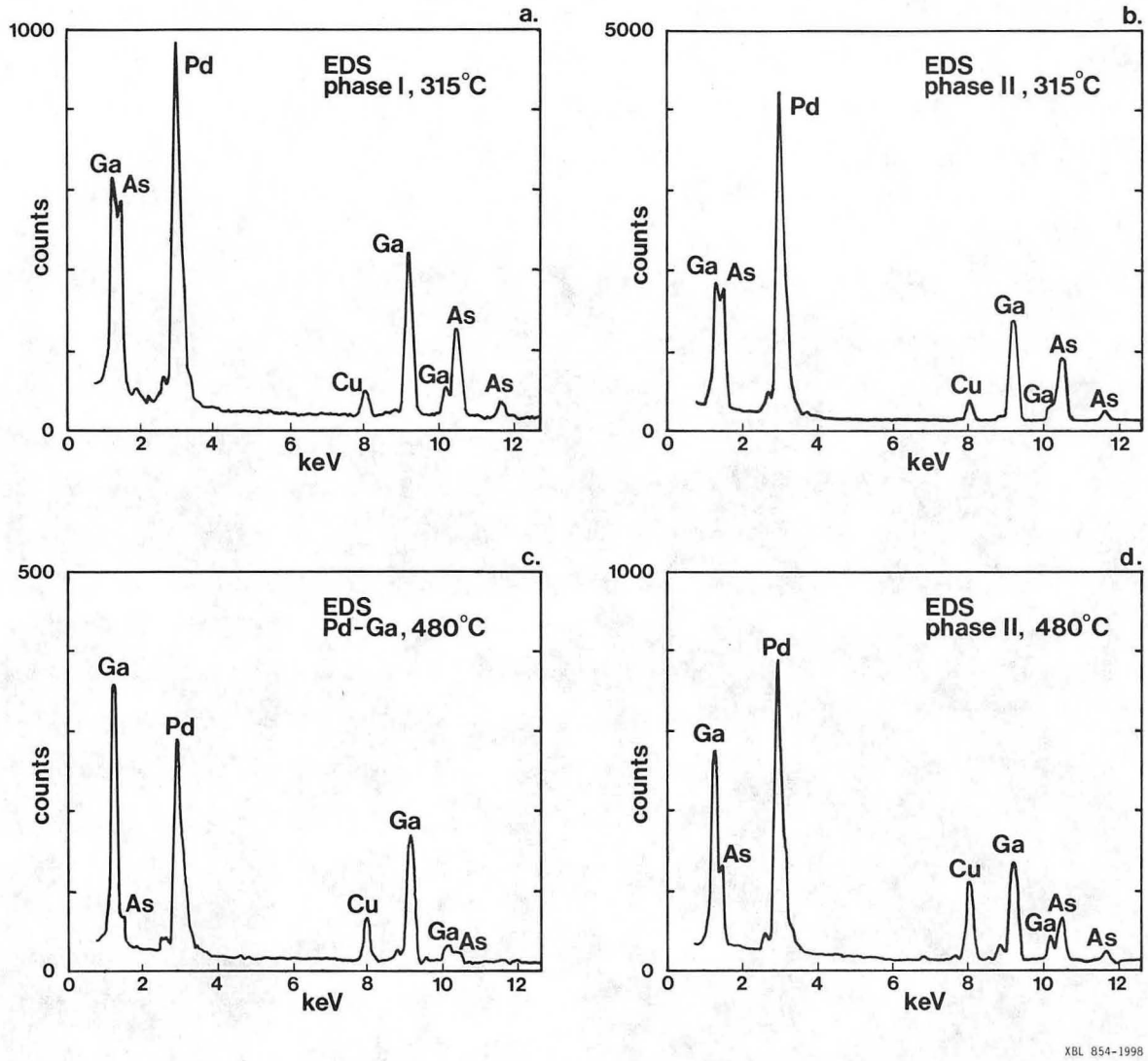
a.
EDS
phase I, 315°C
Pd
Ga
As
Ga
As
Cu
Ga
As
counts
keV
b.
EDS
phase II, 315°C
Pd
Ga
As
Ga
As
Cu
Ga
As
counts
keV
c.
EDS
Pd-Ga, 480°C
Ga
Pd
As
Cu
Ga
Ga
As
counts
keV
d.
EDS
phase II, 480°C
Pd
Ga
As
Cu
Ga
Ga
As
As
counts
keV
XBL 854-1998

Fig. 9

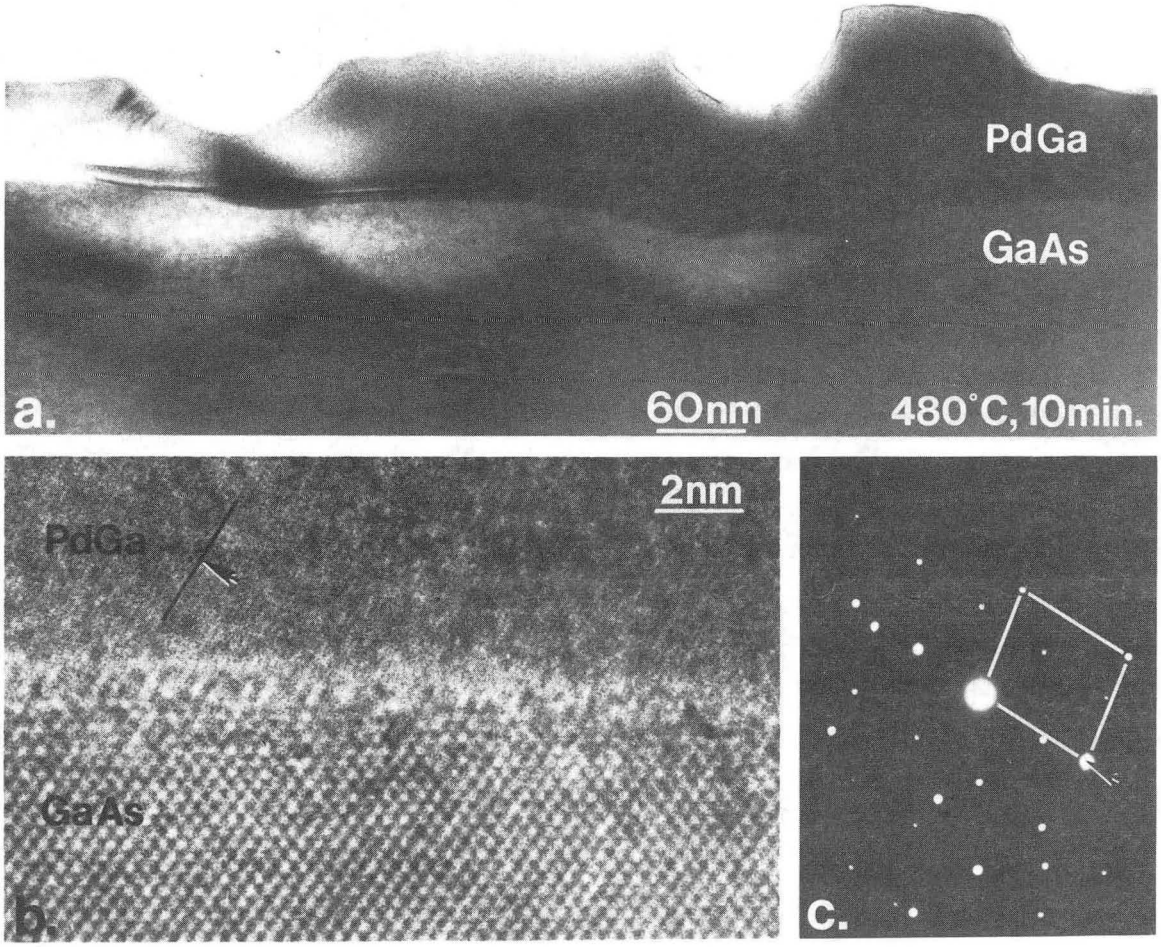

XBB 854-2569

Fig. 10

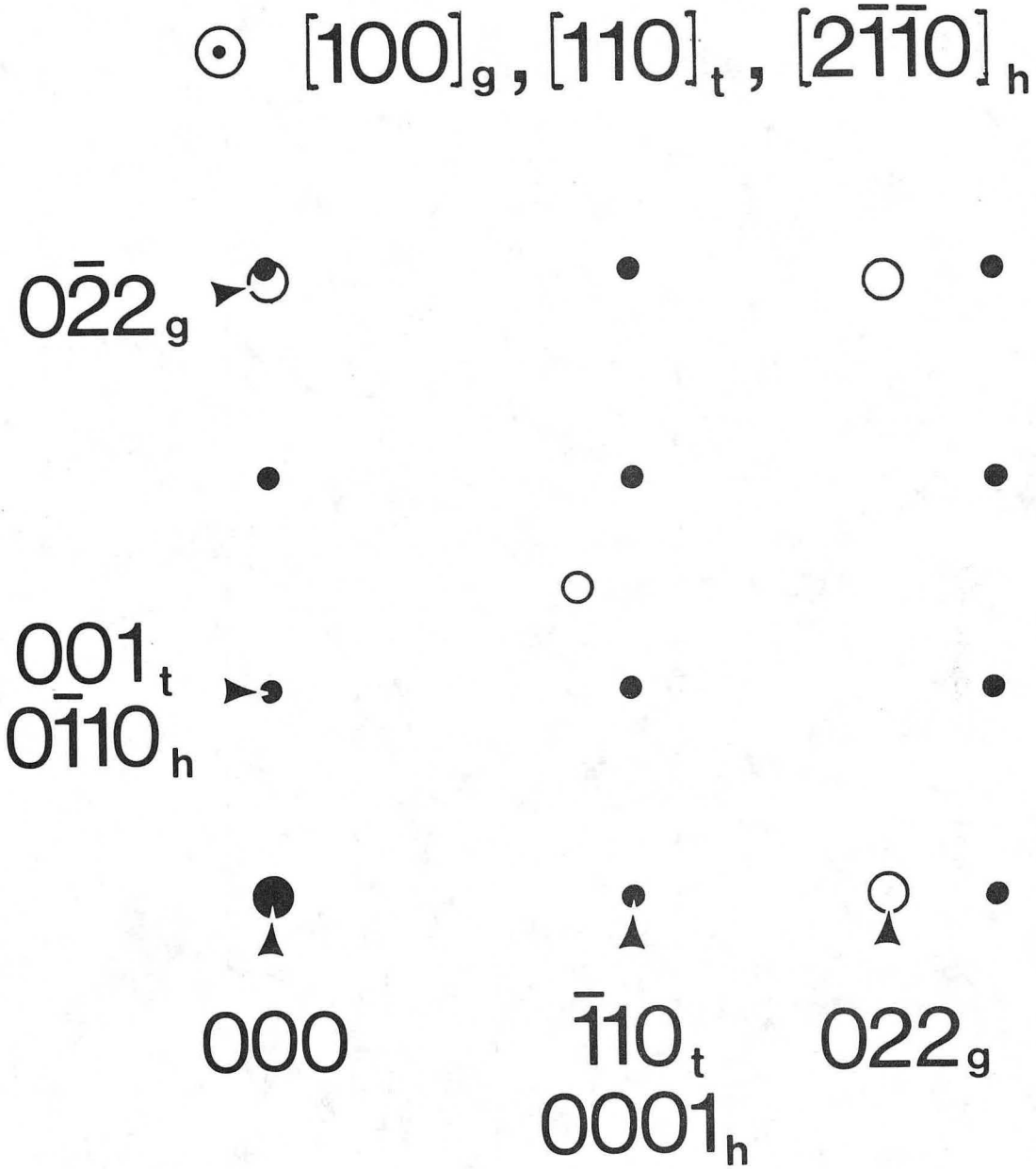

XBL 852-1194

Fig. 11

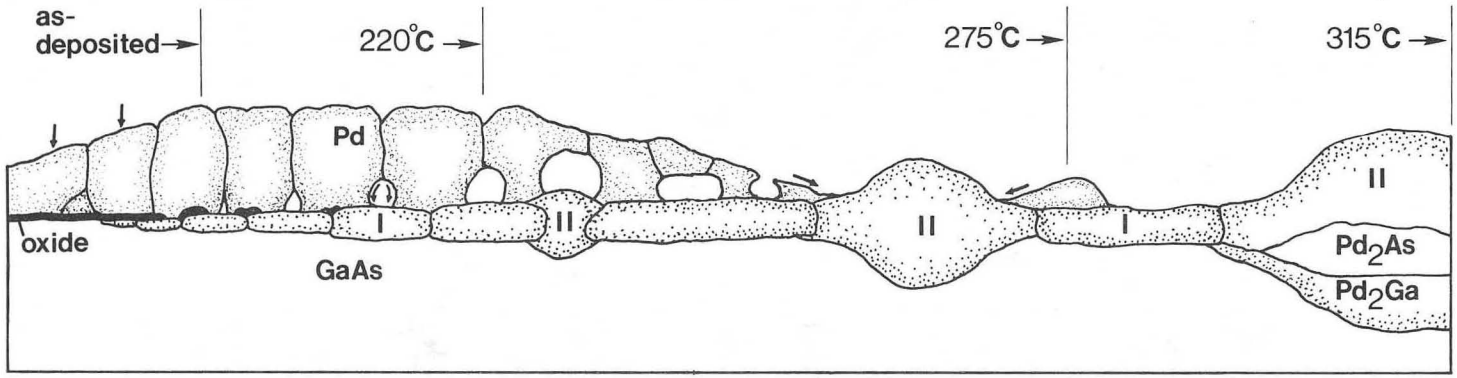

XBL 852-1193

Fig. 12

This report was done with support from the Department of Energy. Any conclusions or opinions expressed in this report represent solely those of the author(s) and not necessarily those of The Regents of the University of California, the Lawrence Berkeley Laboratory or the Department of Energy.

Reference to a company or product name does not imply approval or recommendation of the product by the University of California or the U.S. Department of Energy to the exclusion of others that may be suitable.

TECHNICAL INFORMATION DEPARTMENT
LAWRENCE BERKELEY LABORATORY
UNIVERSITY OF CALIFORNIA
BERKELEY, CALIFORNIA 94720